anism.[6] The situation is different in the 6 K spectrum of $[NH_3]Br_4\cdot4H_2O$. Due to the very small ground-state splitting, all the ground levels are populated at 6 K, and as a result both mechanisms contribute to the intensity at this temperature. As a consequence, the predominance of x polarization is not as pronounced as in $[en]Br_4\cdot2H_2O$.

It is interesting to compare the spectroscopic behavior of [en] and $[NH_3]$ with that found in $Cs_3Cr_2Br_9$[19] on the one hand and $[(NH_3)_5CrOHCr(NH_3)_5]Cl_5\cdot3H_2O$[20] on the other. In $Cs_3Cr_2Br_9$ the chromium dimer has, as in [en] and $[NH_3]$, a center of inversion while in rhodo chromium chloride it has not. In the former case strong contributions to the ^2E, $^2T_1$ intensity from a single ion mechanism have been found[19] while the most intense features in the pair spectrum of rhodo chromium chloride are due to a pair mechanism.[20] Theoretically the Tanabe pair mechanism is expected to be more efficient in the absence of a center of inversion.[21] The experimental evidence so far appears to be in good agreement with that prediction.

A detailed analysis of the spin-forbidden excitations will be published separately.[6]

Acknowledgment. We have profited from the communication of unpublished synthetic and structural information on the NH_3 compounds by Johan Springborg and Erik Pedersen. This work was supported by the Swiss National Science Foundation (Grant No. 2.872-77).

Registry No. $[(NH_3)_4Cr(OH)_2Cr(NH_3)_4]Br_4\cdot4H_2O$, 67326-98-1; $[(NH_3)_4Cr(OH)_2Cr(NH_3)_4]Cl_4\cdot4H_2O$, 51456-44-1; $[(en)_2Cr(OH)_2Cr(en)_2]Br_4\cdot2H_2O$, 15135-03-2; $[(en)_2Cr(OH)_2Cr(en)_2]Cl_4\cdot2H_2O$, 51456-44-1; $[(NH_3)_4Cr(OH)_2Cr(NH_3)_4](ClO_4)_4\cdot2H_2O$, 67326-99-2.

---

(19) Dubicki, L.; Ferguson, J.; Harrowfield, B. *Mol. Phys.* **1977**, *34*, 1545.

(20) Engel, P.; Güdel, H. U. *Inorg. Chem.* **1977**, *16*, 1589.

(21) Gondaira, K.; Tanabe, Y. *J. Phys. Soc. Jpn.* **1966**, *21*, 1527.

Contribution from the Department of Chemistry,
Purdue University, West Lafayette, Indiana 47907

Kinetics of Nickel(II) Glycylglycyl-L-histidine Reactions with Acids and Triethylenetetramine

CHARLES E. BANNISTER, JOHN M. T. RAYCHEBA, and DALE W. MARGERUM*

Received May 15, 1981

Dissociation of the doubly deprotonated glycylglycyl-L-histidine complex of nickel(II), $Ni(H_{-2}GGHis)^-$, occurs by proton-assisted and general-acid (HB) pathways. At pH 5-7 protonation of the second peptide nitrogen is the rate-limiting step as shown by contributions of $[H^+]^2$ and $[H^+][HB]$ terms to the rate. At high HB concentrations, the first protonation step becomes rate limiting. Below pH 5 the dissociation reaction is preceded by the formation of the outside-protonated species $Ni(H_{-2}GGHis)H$ and $Ni(H_{-2}GGHis)2H^+$, in which the peptide oxygens have protonation constants of $10^{4.3}$ M^{-1} and $10^{1.3}$ M^{-1}, respectively. trien (triethylenetetramine) acts as a nucleophile in a proton-assisted pathway at pH 5-8. Comparison with the reactions of $Ni(H_{-2}triglycinate)^-$ shows that the terminal histidyl group decreases the nucleophilic reactions of trien by more than 5 orders of magnitude. The terminal histidyl group also gives rate constants for the proton-transfer reactions of general acids which are 2-3 orders of magnitude smaller; however, the H_3O^+ rate constant (3.0×10^4 M^{-1} s^{-1}) is only a factor of 3 smaller.

Introduction

Kinetic studies of the acid dissociation of nickel(II) peptide complexes[1-6] have shown the presence of two reaction pathways. Direct peptide nitrogen protonation (Scheme I) is general-acid catalyzed. In the other reaction pathway (Scheme II), rapid peptide oxygen protonation is followed by the rate-determining metal-nitrogen bond rupture. More than one proton can add in the outside-protonation reactions. Recent work[3] has shown that the pathways can become mixed with general-acid attack on the outside-protonated species. In general the triply deprotonated peptide complexes $Ni(H_{-3}G_4)^{2-}$, $Ni(H_{-3}G_3a)^-$, and $Ni(H_{-3}G_4a)^-$ (G, glycyl; a, amide) react by the outside-protonation pathway,[2,4,5,6] whereas, the doubly deprotonated peptide complex $Ni(H_{-2}G_3)^-$ reacts by the inside-protonation pathway.[2,4]

Scheme I. Inside Protonation Pathway

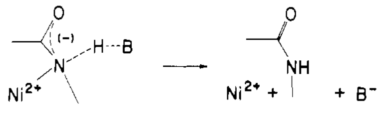

Scheme II. Outside Protonation Pathway

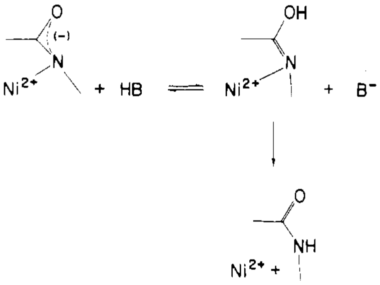

When histidine is the third amino acid in the tripeptide, the imidazole group coordinates in preference to the carboxylate group as shown for $Ni(H_{-2}GGHis)^-$ in structure I. The present work examines the effect of this coordination on the

---

(1) Billo, E. J.; Margerum, D. W. *J. Am. Chem. Soc.* **1970**, *92*, 6811.

(2) Paniago, E. B.; Margerum, D. W. *J. Am. Chem. Soc.* **1972**, *94*, 6704.

(3) Bannister, C. E.; Margerum, D. W. *Inorg. Chem.* **1981**, *20*, 3149.

(4) Bannister, C. E.; Youngblood, M. P.; Young, D. C.; Margerum, D. W., to be submitted for publication.

(5) Raycheba, J. M. T.; Margerum, D. W. *Inorg. Chem.* **1980**, *19*, 497.

(6) Raycheba, J. M. T.; Margerum, D. W. *Inorg. Chem.* **1980**, *19*, 837.

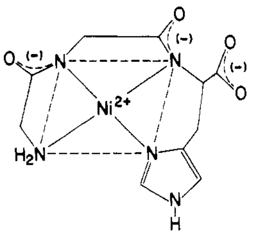

I

kinetics and mechanism of the reactions of the $Ni(H_{-2}GGHis)^-$ complex with acids and with triethylenetetramine (trien). The pH dependence of the rate constant becomes quite complex (Figure 1), and the overall rate of acid decomposition is much slower than is the case for $Ni(H_{-2}G_3)^-$. The susceptibility of $Ni(H_{-2}GGHis)^-$ to nucleophilic attack by trien is greatly reduced when compared with that of the $Ni(H_{-2}G_3)^-$ complex.[7] Both the trien and the acid decomposition reactions are subject to general-acid catalysis. One consequence is that the rate changes with each set of buffer conditions as well as with pH. General-acid catalysis was observed[8-10] for the reactions of trien with $Cu(H_{-2}GGHis)^-$ and a proton-assisted nucleophilic pathway was proposed. A proton assisted-trien pathway is observed for $Ni(H_{-2}GGHis)^-$, but there is also a proton-assisted general-acid pathway.

Experimental Section

Reagents. Nickel(II) perchlorate was prepared from nickel(II) carbonate and perchloric acid. Stock solutions of $Ni(ClO_4)_2$ were standardized with EDTA with a murexide indicator. Solutions of nickel(II) glycylglycyl-L-histidine [$Ni(H_{-2}GGHis)^-$] were prepared by addition of the chromatographically pure glycylglycyl-L-histidine in 10% excess to $Ni(ClO_4)_2$. The yellow complex formed when the pH was slowly adjusted to 8.0–8.5. The ionic strength was maintained at 1.0 with $NaClO_4$, which was prepared from Na_2CO_3 and perchloric acid.

Triethylenetetramine (trien) was prepared as the free base by the slow addition of solid NaOH to a slurry of the disulfate salt of trien in ethanol. After removal of the solid Na_2SO_4, the trien–ethanol mixture was vacuum distilled and the trien fraction boiling at 105–110 °C (0.5 mmHg) was collected. The liquid trien was further purified by an additional vacuum distillation. Stock solutions of trien were standardized with $Cu(ClO_4)_2$ with the PAN indicator.

pH Measurement. All pH readings were thermostated at 25.0 ± 0.1 °C. The relationship between $-\log [H^+]$ and pH (reading) was experimentally determined by titration of $HClO_4$ and NaOH (Sargent-Welch electrodes, saturated NaCl reference) and is given by $-\log [H^+] = pH + 0.30$ for 1.0 M $NaClO_4$.

Kinetic Measurements. The rate of disappearance of $Ni(H_{-2}GGHis)^-$ was followed spectrophotometrically at 245 nm ($\epsilon = 8 \times 10^3\ M^{-1}\ cm^{-1}$) with a Durrum stopped-flow spectrophotometer interfaced to a HP2115A digital computer.[11] With excess buffer and constant pH, excellent pseudo-first-order reactions were observed. On-line linear and nonlinear regression analyses that used eq 1 and

$$A - A_\infty = (A_0 - A_\infty)e^{-k_{obsd}t} \qquad (1)$$

data covering at least 3 half-lives of the reaction were employed to evaluate the initial absorbance (A_0), the final absorbance (A_∞), and the observed pseudo-first-order rate constant (k_{obsd}). All reported rate constants were determined in 1.0 M $NaClO_4$ at 25.0 °C. The k_{obsd} values are the average of at least three replicates and their standard deviations are given.

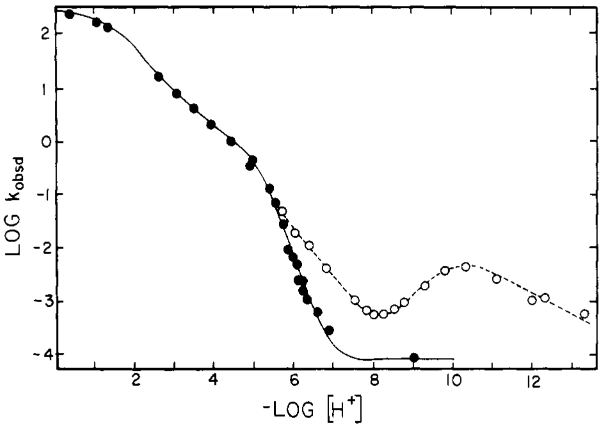

Figure 1. pH dependence of the observed dissociation rate constant in the absence (●) and the presence (○) of excess trien (0.0676 M). The solid curve was calculated from eq 14 and the kinetic constants given in Table VI.

Table I. Observed Rate Constants for the Reaction of $Ni(H_{-2}GGHis)^-$ with H_3O^+ (1.0 M $NaClO_4$, 25.0 °C)[a]

$-\log [H^+]$	k_{obsd}, s^{-1}	$-\log [H^+]$	k_{obsd}, s^{-1}
0.30	212 ± 5	5.57	$(5.80 \pm 0.02) \times 10^{-2}$
1.00	152 ± 5	5.74	$(2.73 \pm 0.04) \times 10^{-2}$
1.30[b]	113 ± 4	5.82	$(6.58 \pm 0.01) \times 10^{-3}$
2.61	14.4 ± 0.1	5.86[c]	$(6.17 \pm 0.05) \times 10^{-3}$
3.00	7.33 ± 0.04	6.03	$(4.60 \pm 0.05) \times 10^{-3}$
3.45	3.63 ± 0.02	6.09	$(2.21 \pm 0.02) \times 10^{-3}$
3.88	1.80 ± 0.01	6.12	$(2.28 \pm 0.05) \times 10^{-3}$
4.36	0.856 ± 0.005	6.20	$(1.43 \pm 0.04) \times 10^{-3}$
4.85	0.315 ± 0.004	6.28	$(1.03 \pm 0.02) \times 10^{-3}$
4.87	0.402 ± 0.002	6.51	$(6.0 \pm 0.3) \times 10^{-4}$
5.39	0.105 ± 0.001	6.93[d]	$(2.7 \pm 0.2) \times 10^{-4}$

[a] $[Ni(H_{-2}GGHis)^-]_T = 2.5 \times 10^{-5}$ M. [b] $-\log [H^+] < 1.30$, $HClO_4$ used. [c] $-\log [H^+] < 5.86$, $[HOAc]_T = [formic]_T = [ClCH_2CO_2H]_T = 0.01$ M. [d] $-\log [H^+] < 6.93$, $[MES]_T = 0.010$ M, $[trien]_T = 1.0 \times 10^{-4}$ M. See ref 18.

Table II. Observed Rate Constants for the Reaction of $Ni(H_{-2}GGHis)^-$ with H_3O^+ in the Presence of 0.0676 M $[trien]_T$ (1.0 M $NaClO_4$, 25.0 °C)[a]

$-\log [H^+]$	$10^3 k_{obsd}$, s^{-1}	$-\log [H^+]$	$10^3 k_{obsd}$, s^{-1}
5.63[b]	41.9 ± 0.1	8.80	0.87 ± 0.02
6.03[b]	16.8 ± 0.2	9.27	1.76 ± 0.05
6.36	10.4 ± 0.1	9.80	3.50 ± 0.02
6.82	3.76 ± 0.03	10.26	4.16 ± 0.02
7.55	0.93 ± 0.01	11.11	2.69 ± 0.04
7.79	0.63 ± 0.02	12.0[c]	1.04 ± 0.04
8.02	0.551 ± 0.008	12.3[c]	1.14 ± 0.03
8.28	0.530 ± 0.006	13.0[c]	0.53 ± 0.03
8.53	0.67 ± 0.03		

[a] $[Ni(H_{-2}GGHis)^-]_T = 2.5 \times 10^{-5}$ M. [b] 0.020 M $[MES]_T$; see ref 18. [c] NaOH used.

Results and Discussion

The stoichiometric reaction for the acid decomposition of $Ni(H_{-2}GGHis)^-$ is given by eq 2, where L represents the

$$Ni(H_{-2}L)^- + 4H^+ \rightarrow Ni^{2+}(aq) + H_2L^+ \qquad (2)$$

glycylglycyl-L-histidine anion. In the presence of trien the final product is $Ni(trien)^{2+}$. The overall reaction involves the dissociation of a ligand, the protonation of two peptide nitrogens, and a change in the nickel(II) geometry from square planar to octahedral. In these respects the $Ni(H_{-2}L)^-$ acid decomposition reaction is similar to the acid dissociation reactions of the nickel(II) triglycine,[1,3] tetraglycine, triglycinamide,[2,4] and tetraglycinamide.[5]

---

(7) Billo, E. J.; Smith, G. F.; Margerum, D. W. *J. Am. Chem. Soc.* **1971**, *93*, 2635.

(8) Wong, L. F.; Cooper, J. C.; Margerum, D. W. *J. Am. Chem. Soc.* **1976**, *98*, 7268.

(9) Cooper, J. C.; Wong, L. F.; Venezky, D. L.; Margerum, D. W. *J. Am. Chem. Soc.* **1974**, *96*, 7560.

(10) Bannister, C. E.; Margerum, D. W.; Raycheba, J. M. T.; Wong, L. F. *Symp. Faraday Soc.* **1975**, *No. 10*, 78.

(11) Willis, B. G.; Bittikoffer, J. A.; Pardue, H. L.; Margerum, D. W. *Anal. Chem.* **1970**, *42*, 1340.

Table III. pH and trien Dependence of the Observed Pseudo-First-Order Rate Constant for the Reaction of $Ni(H_{-2}GGHis)^-$ with trien[a]

$[trien]_T$, M	$-\log [H^+]$	10^2k_{obsd}, s^{-1}
0.004 89	6.30	0.318 ± 0.002
0.0195	6.30	0.715 ± 0.003
0.0293	6.30	0.795 ± 0.002
0.0489	6.34	0.882 ± 0.004
0.0676	6.36	1.04 ± 0.02
0.007 50	7.14	0.068 ± 0.002
0.009 57	7.14	0.075 ± 0.002
0.0191	7.17	0.116 ± 0.002
0.0383	7.17	0.146 ± 0.003
0.0479	7.18	0.159 ± 0.002
0.0574	7.17	0.172 ± 0.002
0.00745	9.28	0.202 ± 0.003
0.0186	9.28	0.053 ± 0.001
0.0372	9.32	0.109 ± 0.002
0.0559	9.28	0.157 ± 0.003
0.0676	9.27	0.176 ± 0.002
0.004 89[b]	6.28	0.576 ± 0.001
0.0195[b]	6.29	0.858 ± 0.002
0.0391[b]	6.30	0.998 ± 0.003
0.004 89[c]	6.29	0.762 ± 0.001
0.0195[c]	6.28	1.02 ± 0.01
0.0391[c]	6.29	1.13 ± 0.01

[a] Conditions: $[Ni(H_{-2}GGHis)^-]_T = 2.5 \times 10^{-5}$ M; $\mu = 1.0$ M ($NaClO_4$); 25.0 °C; 0.01 M $[MES]_T$ or 0.01 M $[PIPES]_T$.[18] [b] 0.010 M $[CH_3CO_2H]_T$. [c] 0.02 M $[CH_3CO_2H]_T$.

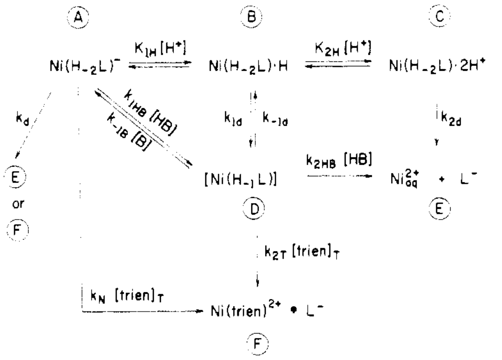

Figure 2. Summary of the $Ni(H_{-2}GGHis)^-$ decomposition pathways. In the following assignments, the arrow (→) indicates the location(s) of the rate-determining step(s) for each reaction pathway, and all subsequent reaction steps can be considered to be rapid. (a) Nucleophilic: A → F. (b) Outside-protonation: AB → DE; ABC → E. (c) Proton-assisted nucleophilic: AB → D → F; A → D → F. Proton-assisted general-acid: AB → D → E; A → D → E. (e) Inside-protonation: A → DE.

The rate of disappearance of $Ni(H_{-2}L)^-$ was studied under pseudo-first-order conditions and was consistent with the rate law given by eq 3, where k_{obsd} is a function of the pH (Tables I, II), the trien concentration (Tables II, III), and the general-acid (HB) concentration (Tables IV, V). A summary of the pathways for the reaction of $Ni(H_{-2}GGHis)^-$ with trien and with acids is shown in Figure 2.

$$-\frac{d[Ni(H_{-2}L)^-]_T}{dt} = k_{obsd}[Ni(H_{-2}L)^-]_T \qquad (3)$$

Nucleophilic Pathway (pH >8). At $-\log [H^+] = 9.29$, a first-order dependence on the trien concentration is observed (Figure 3a, Table III), and at a constant total trien concentration of 0.067 M, the observed rate constant steadily increases from pH 8 to 10 (Table II). On the basis of the pH dependence, it is concluded that the order of reactivity for the various trien species is trien > $H(trien)^+$ > $H_2(trien)^{2+}$. This reactivity order is consistent with a reaction sequence in which the polyamine, trien, is behaving as a nucleophile in its reaction with $Ni(H_{-2}GGHis)^-$. A similar nucleophilic reaction pathway has been observed for the reaction of trien and other polyamine and aminocarboxylate ligands with Ni(II)- and Cu(II)-de-

Table IV. Effect of General Acids on the $Ni(H_{-2}GGHis)^-$ Acid Dissociation Rate[a]

$[HB]_T$, M	$-\log [H^+]$	10^2k_{obsd}, s^{-1}
	HB = H_2(glycinate)$^+$ [b]	
0	5.81	0.791 ± 0.002
0.0050	5.81	0.886 ± 0.004
0.010	5.81	0.985 ± 0.003
0.030	5.83	1.29 ± 0.02
0.050	5.79	1.57 ± 0.02
0.10	5.82	2.01 ± 0.02
0.20	5.82	2.68 ± 0.01
	HB = HOAc[b]	
0.050	4.87	40.2 ± 0.2
0.10	4.84	43.2 ± 0.1
0.20	4.86	48.8 ± 0.2
0.25	4.86	51.8 ± 0.2
0.005	5.85	2.19 ± 0.01
0.010	5.85	2.79 ± 0.02
0.030	5.85	3.94 ± 0.03
0.050	5.79	6.14 ± 0.02
0.10	5.83	5.19 ± 0.01
0.15	5.79	6.14 ± 0.02
0.20	5.78	6.82 ± 0.04
0	6.26	0.109 ± 0.001
0.010	6.24	0.529 ± 0.003
0.020	6.26	0.750 ± 0.004
0.030	6.26	0.933 ± 0.002
0.040	6.24	1.09 ± 0.01
0.10	6.28	1.58 ± 0.01
0.15	6.31	1.79 ± 0.01
0.20	6.31	2.09 ± 0.02
0.25	6.30	2.39 ± 0.01
0.010[d]	6.32	1.08 ± 0.01
0.020[d]	6.32	1.19 ± 0.01
0.050[d]	6.30	1.40 ± 0.01
0.20[d]	6.31	2.22 ± 0.01
	HB = NH_3OH^+ [b]	
0.0050	5.84	1.11 ± 0.02
0.010	5.81	1.34 ± 0.02
0.030	5.82	2.24 ± 0.02
0.050	5.83	3.01 ± 0.01
0.10	5.83	4.63 ± 0.01
0.15	5.86	6.03 ± 0.03
0.25	5.83	8.50 ± 0.04

[a] Conditions: $[Ni(H_{-2}GGHis)^-]_T = 2.5 \times 10^{-5}$ M; $\mu = 1.0$ M ($NaClO_4$); 25.0 °C. [b] $[MES]_T = 0.02$ M; $[trien]_T = 1.0 \times 10^{-4}$ M. [c] $[MES]_T = 0.10$ M. [d] $[trien]_T = 0.0586$ M.

Table V. Additive Effect of Acetic Acid and Other General Acids on the $Ni(H_{-2}GGHis)^-$ Acid Dissociation Rate[a]

$[HB]_T$, M	$-\log [H^+]$	10^2k_{obsd}, s^{-1}
	HB = H_2(glycinate)$^+$	
0.030	5.82	5.48 ± 0.05
0.050	5.80	5.70 ± 0.05
0.10	5.79	6.01 ± 0.07
0.15	5.82	5.86 ± 0.03
	HB = HCOOH	
0	5.79	5.70 ± 0.01
0.050	5.80	5.89 ± 0.02
0.10	5.81	6.02 ± 0.01
0.15	5.81	6.24 ± 0.02
0.20	5.81	6.54 ± 0.02
	HB = NH_3OH^+	
0.020	5.82	5.91 ± 0.02
0.050	5.82	6.30 ± 0.02
0.10	5.81	7.54 ± 0.03
0.13	5.81	8.31 ± 0.01

[a] Conditions: $[Ni(H_{-2}GGHis)^-]_T = 2.5 \times 10^{-5}$ M; $\mu = 1.0$ M ($NaClO_4$); 25.0 °C; [trien] = 1.0×10^{-4} M; $[MES]_T = 0.02$ M; $[CH_3CO_2H]_T = 0.10$ M.

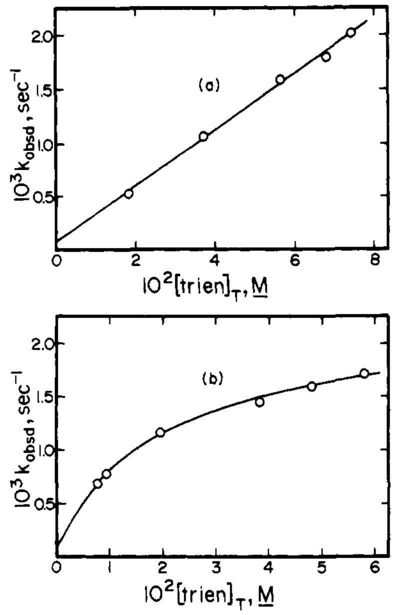

Figure 3. trien dependence of the $Ni(H_{-2}GGHis)^-$ reaction with trien at $-\log [H^+]$ equal to (a) 9.29 and (b) 7.16. The curve in (b) was calculated from eq 19 and the rate constants given in Tables VI and VII.

protonated peptide complexes.[7,9,12,13]

The mechanism proposed to account for the reaction of $Ni(H_{-2}GGHis)^-$ and trien above pH 8 is given in eq 4–7. At constant pH, the trien dependence of the observed rate constant is given by eq 8, where $k_N = (k_T[\text{trien}] + k_{HT}[\text{Htrien}^+] + k_{H_2T}[\text{H}_2\text{trien}^{2+}])/[\text{trien}]_T$.

$$Ni(H_{-2}L)^- + H_2O + trien_T \xrightarrow{k_N} Ni(H_{-1}L)(trien) + OH^- \qquad (4)$$

$$Ni(H_{-1}L)(trien) + H_2O \xrightarrow{\text{rapid}} Ni(trien)^{2+} + OH^- + L^- \qquad (5)$$

$$Ni(H_{-2}L)^- + H_2O \xrightarrow{k_d} Ni(H_{-1}L) + OH^- \qquad (6)$$

$$Ni(H_{-1}L) + trien_T + H_2O \xrightarrow{\text{rapid}} Ni(trien)^{2+} + OH^- + L^- \qquad (7)$$

$$k_{obsd} = k_d + k_N[\text{trien}]_T \qquad (8)$$

Above pH 10.5, hydroxide inhibition of the nucleophilic reaction with trien is observed (Figure 1, Table II). Such behavior may be due to (a) the reversibility of eq 4 at high $[OH^-]$ so that the rate-limiting step is shifted to the decomposition of the mixed complex (eq 5) or (b) an additional deprotonation of $Ni(H_{-2}L)^-$ to give a $Ni(H_{-3}L)^{2-}$ complex, which is less susceptible to a nucleophilic reaction with trien.

Deprotonation of the pyrrole nitrogen in the CH_3HgIm (Im = imidazole) complex has been observed,[14] and a similar deprotonation could occur with the $Ni(H_{-2}GGHis)^-$ complex. However, the absorption spectra (200–600 nm) of $Ni(H_{-2}GGHis)^-$ are identical at pH 9.5 and 13 and it is unlikely that a less reactive form of the Ni^{2+}GGHis complex is formed in appreciable concentration at high pH. Consequently, the hydroxide rate suppression observed above pH 10.5 is attributed to a shift of the rate-determining step from eq 4 to eq 5.

The resolved value of the solvent dissociation rate constant, k_d (eq 6), is 8×10^{-5} s^{-1}. This is 3 orders of magnitude smaller than the k_d value (0.086 s^{-1}) that has been measured for the dissociation of the $Ni(H_{-2}G_3)^-$ complex.[3] Similarly, at $-\log [H^+] = 9.29$, k_N is 2.6×10^{-2} M^{-1} s^{-1}, while the analogous rate constant for the reaction of trien with $Ni(H_{-2}G_3)^-$ is 4×10^5 times larger at the same pH.[7] Thus, the presence of a coordinated terminal imidazole group in $Ni(H_{-2}GGHis)^-$ complex (structure I) compared with the terminal carboxylate group in $Ni(H_{-2}G_3)^-$ reduces the rate of the solvent dissociation and trien nucleophilic reactions by 3 and 5 orders of magnitude, respectively. This supports the earlier conclusion that displacement of the terminal group of the peptide is important in the nucleophilic reactions of metal-deprotonated peptide complexes.[7]

Acid-Dissociation Reactions. Outside-Protonation Pathway. The observed first-order rate constant for the acid decomposition of $Ni(H_{-2}GGHis)^-$ as a function of pH is shown in Figure 1. The rate dependence on the H_3O^+ concentration changes from second order between $-\log [H^+] = 7$ and 5 to zero order at $-\log [H^+] < 1$. When trien is present, a first-order rather than a second-order $[H^+]$ dependence is observed between pH 5.5 and 7.5. This change in the reaction rate order is indicative of a mechanism that involves a shift in the location of the rate-determining step when scavengers such as trien are present.

A mechanism that is consistent with the pH profile (Figure 1) is given in eq 6 and 9–13. Equations 9 and 11 are rapid outside protonation reactions in which a peptide oxygen is protonated (structure II) prior to the rate-limiting cleavage of the nickel(II)–N(peptide) bond (eq 10 and 12). The formation of outside protonated species similar to $Ni(H_{-2}GGHis)\cdot H$ (eq 9, structure II) and $Ni(H_{-2}GGHis)\cdot 2H^+$ have been proposed for a number of other metal–peptide complexes.[2,5,6] Reactions that proceed by an outside-protonation pathway such as that given in eq 9–12 are specific acid rather than general acid catalyzed.

$$Ni(H_{-2}L)^- + H^+ \overset{K_{1H}}{\rightleftharpoons} Ni(H_{-2}L)\cdot H \qquad (9)$$

$$Ni(H_{-2}L)\cdot H \underset{k_{-1d}}{\overset{k_{1d}}{\rightleftharpoons}} Ni(H_{-1}L) \qquad (10)$$

$$Ni(H_{-2}L)\cdot H + H^+ \overset{K_{2H}}{\rightleftharpoons} Ni(H_{-2}L)\cdot 2H^+ \qquad (11)$$

$$Ni(H_{-2}L)\cdot 2H^+ \xrightarrow{k_{2d}} Ni^{2+} + L^- \qquad (12)$$

$$Ni(H_{-1}L) + H^+ \xrightarrow{k_{2H}} Ni^{2+} + L^- \qquad (13)$$

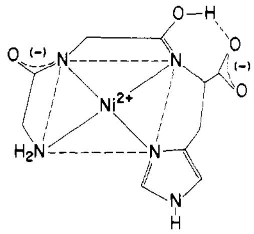

II

The observed pseudo-first-order rate constant that accounts for the outside-protonation reaction pathway (eq 6, 9–13) is given in eq 14. In the presence of a large excess of trien at pH >5, the $Ni(H_{-1}L)$ species produced by reactions 6 and 10 is scavenged by trien (eq 7). Under these conditions the

$$k_{obsd} = \frac{k_d + \dfrac{K_{1H}k_{1d}k_{2H}[H^+]^2}{k_{-1d} + k_{2H}[H^+]} + K_{1H}K_{2H}k_{2d}[H^+]^2}{1 + K_{1H}[H^+] + K_{1H}K_{2H}[H^+]^2} \qquad (14)$$

---

(12) Pagenkopf, G. K.; Margerum, D. W. *J. Am. Chem. Soc.* **1970**, *92*, 2683.
(13) Hauer, H.; Dukes, G. R.; Margerum, D. W. *J. Am. Chem. Soc.* **1973**, *95*, 3515.
(14) Evans, C. A.; Rabenstein, D. L.; Geier, G.; Erni, I. W. *J. Am. Chem. Soc.* **1977**, *99*, 8106.

Table VI. Outside-Protonation Constants and Rate Constants for $Ni(H_{-2}GGHis)^-$, $Ni(H_{-3}G_4)^{2-}$, and $Ni(H_{-3}G_4a)^-$

constant	$Ni(H_{-2}GGHis)^{-\,a}$	$Ni(H_{-3}G_4)^{2-\,b}$	$Ni(H_{-3}G_4a)^{-\,a,c}$
k_d, s^{-1}	8×10^{-5}	1.6×10^{-5}	8×10^{-5}
k_{1d}, s^{-1}	1.5	5.6	12
K_{1H}, M^{-1}	$10^{4.3}$	$10^{4.25}$	$10^{2.4}$
$K_{1H}k_{1d}$, $M^{-1}\ s^{-1}$	3.0×10^4	9.9×10^4	3.2×10^3
k_{2H}/k_{-1d}, M^{-1}	1.3×10^5		
k_{2d}, s^{-1}	250		43
K_{2H}, M^{-1}	$10^{1.3}$	$\simeq 10^{1.5}$	$10^{1.3}$

[a] $\mu = 1.0$ M ($NaClO_4$). [b] $\mu = 0.10$ M ($NaClO_4$); ref 2 and 4. [c] Reference 5.

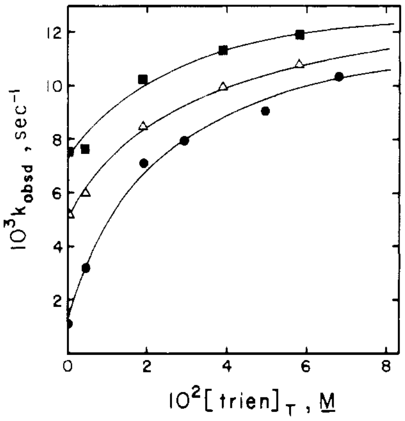

Figure 4. trien dependence of the $Ni(H_{-2}GGHis)^-$ reaction with trien at $-\log [H^+] = 6.23$ and total acetic acid concentrations of (●) 0, (▲) 0.010, and (■) 0.020 M. The solid curves were calculated from eq 22 and the resolved constants given in Tables VI and VII.

rate-determining step is shifted to eq 10 and 12, $K_{1H}K_{2H}k_{2d}[H^+]$ is much less than $K_{1H}k_{1d}$, eq 14 simplifies to eq 15, and

$$k_{obsd} = k_d + K_{1H}k_{1d}[H^+] \qquad (15)$$

as has been noted, a first-order $[H^+]$ dependence is observed (Figure 1, Table II). In the absence of a scavenger at pH 5–7, eq 12 and 13 become rate-determining and the expression for the observed rate constant is given by eq 16, which is consistent with the second-order $[H^+]$ dependence that is observed (Figure 1, Table I).

$$k_{obsd} = k_d + (K_{1H}k_{1d}k_{2H}/k_{-1d} + K_{1H}K_{2H}k_{2d})[H^+]^2 \qquad (16)$$

The data in Table I were used to obtain the resolved values of the rate and equilibrium constants listed in Table VI. These constants and eq 14 were used to calculate the solid line in Figure 1.

The values of the first outside-protonation constant (K_{1H}) and of k_d for $Ni(H_{-2}GGHis)^-$ are similar to those for $Ni(H_{-3}G_4)^{2-}$ (Table VI). In each case the uncoordinated terminal carboxylate group is capable of forming an internal hydrogen bond (structure II).[2]

Proton-Assisted Nucleophilic Pathway. Between pH 5.5 and 8, the reactions of trien with $Ni(H_{-2}GGHis)^-$ differs from the higher pH reactions in that a limiting rate is approached as the trien concentration is increased (Figures 3 and 4). The value of the limiting rate constant depends on the pH. In these experiments, the initial absorbance at 245 nm, A_0, obtained by extrapolating the absorbance vs. time data to $t = 0$ was the same as the A_0 value expected from simple mixing of the reactant solutions. That is, no absorbance jump was observed prior to the monitored reaction. This observation indicates that the $Ni(H_{-2}L)^-$ species is the only Ni^{II}GGHis-containing reactant that is present in appreciable concentrations, and therefore, the change from a first-order to a zero-order trien dependence must arise as a result of a shift in rate-determining step rather than from a change in reactant.

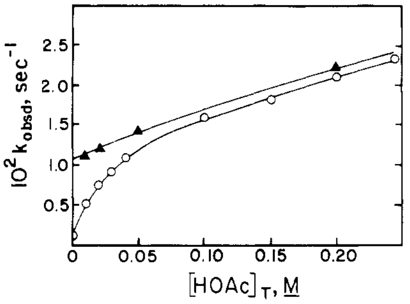

Figure 5. Dependence of k_{obsd} on the concentration of acetic acid at $-\log [H^+] = 6.31$ in the presence of no trien (○) and of 0.0586 M $[trien]_T$ (▲). The solid curves were calculated from eq 22 and the rate constants given in Tables VI and VII.

The mechanism proposed to account for the $[H^+]$ and [trien] dependences between pH 5.5 and 8 is given by eq 6, 9–13, and 17. At constant pH, the trien dependence of the observed rate constant is given by eq 18. At pH 7, eq 18 can be simplified to eq 19. The data in Table III at $-\log [H^+] = 7.16$ and the previously resolved constants from Table VI were used to obtain a value of 49 M^{-1} for the ratio of rate constants k_{2T}/k_{-1d}.

$$Ni(H_{-1}L) + trien_T \xrightarrow{k_{2T}} Ni(trien)^{2+} + L^- + OH^- \qquad (17)$$

$$k_{obsd} = k_d + \frac{K_{1H}k_{1d}k_{2H}[H^+]^2 + K_{1H}k_{1d}k_{2T}[H^+][trien]_T}{k_{-1d} + k_{2H}[H^+] + k_{2T}[trien]_T} \qquad (18)$$

$$k_{obsd} = k_d + \frac{K_{1H}k_{1d}k_{2T}[H^+][trien]_T}{k_{-1d} + k_{2T}[trien]_T} \qquad (19)$$

The solid line in Figure 3b was calculated from eq 19. A similar analysis at $-\log [H^+] = 6.32$ (Figure 4, Table III) resulted in the same value for k_{2T}/k_{-1d}. This indicates that $H_2(trien)^{2+}$ and $H_3(trien)^{3+}$ have similar reactivities with $Ni(H_{-1}L)$ (eq 17). Since $H_3(trien)^{3+}$ is expected to be a much less effective nucleophile than is $H_2(trien)^{2+}$, $H_3(trien)^{3+}$ acts as a general acid rather than as a nucleophile in its reaction with $Ni(H_{-1}GGHis)^-$. On the other hand, $H_2(trien)^{2+}$ which is a much weaker acid than $H_3(trien)^{3+}$, behaves as a nucleophile in its reaction with $Ni(H_{-1}GGHis)^-$.

Therefore, the reaction of $Ni(H_{-2}GGHis)^-$ with trien (eq 3–13, 17) at pH <8 consists of a prior peptide-nitrogen protonation to give $Ni(H_{-1}L)$ followed by a combination of general-acid, $H_3(trien)^{3+}$, and nucleophilic, $H_2(trien)^{2+}$, reactions. This behavior differs from the analogous $Cu(H_{-2}GGHis)^-$ reactions in which the protonation to give $Cu(H_{-1}GGHis)$ is followed only by a nucleophilic reaction with $H_2(trien)^{2+}$.[8,9] That is, the reaction of $Cu(H_{-1}GGHis)$ with the general acid $H_3(trien)^{3+}$ was not observed.[9]

Proton-Assisted General-Acid Reaction. General-acid (HB) reactions with $Ni(H_{-2}GGHis)^-$ are observed in both the presence and absence of trien (Tables III, IV). This is shown in Figure 4 for the reaction of $Ni(H_{-2}GGHis)^-$ with trien in the presence of acetic acid (HOAc). The effect of acetic acid, $H_2(glycinate)^+$, and NH_3OH^+ on the $Ni(H_{-2}GGHis)^-$ dissociation rate in the presence of trien is shown in Figures 5 and 6. For each acid, the rate dependence of the $Ni(H_{-2}GGHis)^-$ decomposition is not first order with respect to the HB concentration and resembles the reaction with trien. This kinetic behavior differs from that of the $Cu(H_{-2}GGHis)^-$ reaction in which general-acid catalysis is observed only in the presence of trien.[8,9] At pH 5 the rate of dissociation of $Cu(H_{-2}GGHis)^-$ is second order in $[H^+]$ and the same behavior is found with

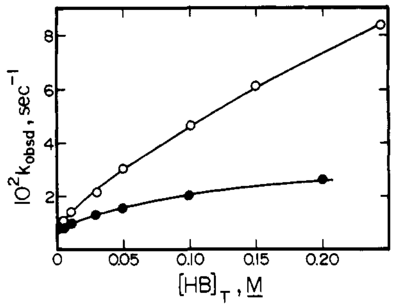

Figure 6. Dependence of k_{obsd} on the concentration of (●) H_2(glycinate)$^+$ (–log $[H^+]$ = 5.81) and (○) NH_3OH^+ (–log $[H^+]$ = 5.83). The solid curves were calculated from eq 22 and the rate constants given in Tables VI and VII.

$Ni(H_{-2}GGHis)^-$, except that there is also a $[H^+][HB]$ rate dependence. It appears that the $Ni(H_{-1}GGHis)$ decomposition reaction is more subject to general-acid catalysis than is the $Cu(H_{-1}GGHis)$ decomposition reaction.

A mechanism consistent with the observed kinetic behavior involves a proton-assisted general-acid pathway (eq 20, 21) in which both $Ni(H_{-2}GGHis)^-$ and $Ni(H_{-1}GGHis)$ react with HB. This mechanism is similar to the proposed pathway for trien reacting with $Cu(H_{-2}GGHis)^-$ (eq 9, 10, 17).

$$Ni(H_{-2}L)^- + HB \underset{k_{-1B}}{\overset{k_{1HB}}{\rightleftharpoons}} Ni(H_{-1}L) + B^- \tag{20}$$

$$Ni(H_{-1}L) + HB \xrightarrow{k_{2HB}} Ni^{2+} + L^- + B^- \tag{21}$$

The first-order rate constant is described by eq 22, where

$$k_{obsd} = k_d + \frac{(K_{1H}k_{1d}[H^+] + k_{1HB}[HB])(k_{2H}[H^+] + k_{2HB}[HB])}{k_{-1d} + k_{-1B}[B] + k_{2H}[H^+] + k_{2HB}[HB]} \tag{22}$$

HB represents all acids in solution with the exception of H_3O^+. At pH 5.5–8 with very low HB concentrations, the observed rate constant, k_{obsd}, is approximately equal to $K_{1H}k_{1d}(k_{2H}/k_{-1d})[H^+]^2$ (Figure 1). That is, in the absence of general acids, the rate of the $Ni(H_{-2}GGHis)^-$ acid dissociation is carried by the outside-protonation pathway (eq 9–12) discussed earlier. At high HB concentrations, both the specific-acid- (eq 9, 10) and the general-acid-catalyzed (eq 20) protonations of $Ni(H_{-2}GGHis)^-$ contribute to the dissociation rate (Figures 5, 6) and the observed pseudo-first-order rate constant simplifies to eq 23.

$$k_{obsd} = k_d + K_{1H}k_{1d}[H^+] + k_{1HB}[HB] \tag{23}$$

The resolved values of k_{1HB} and k_{2HB}/k_{-1d} for acetic acid, H_2(glycinate)$^+$, and NH_3OH^+ were evaluated from the data in Table IV with eq 22 and are given in Table VII. The fraction of the total acid concentration present as HB is given by the ratio, $[H^+]/([H^+] + K_a)$, where K_a is the acid dissociation constant for HB, and under the conditions used, base catalysis of $Ni(H_{-1}L)$ to give $Ni(H_{-2}L)^-$ ($k_{-1B}[B]$ in eq 20) is not observed. The solid lines in Figures 5 and 6 were calculated from eq 22 and the resolved constants given in Table VII. The rate constants, k_{1HB}, for NH_3OH^+, H_2(glycinate)$^+$, and formic acid, which were determined from eq 23 and data obtained in the presence of acetic acid (Table V), were in agreement with the values obtained in the absence of acetic acid.

Table VII. Resolved Rate Constants for the Protonation of $Ni(H_{-2}GGHis)^-$ by HB (1.0 M $NaClO_4$, 25.0 °C)

HB	pK_a	k_{1HB}, M^{-1} s^{-1}	k_{2HB}/k_{-1d}, M^{-1}
H_3O^+	−1.74		1.3×10^5
H_2(glycinate)$^+$	2.45[a]	$<5 \times 10^1$	1.9×10^4
HCOOH	3.75[b]	4.7	
HOAc	4.64[c]	1.95	2.1×10^3
NH_3OH^+	6.06[d]	3.6×10^{-1}	3.2×10^1
H_3(trien)$^{3+}$	7.15[e]		4.9×10^1 [f]
H_2O	15.52	8×10^{-5} [g]	

[a] Mercier, R. C.; Bonnet, M.; Paris, M. R. *Bull. Soc. Chim. Fr.* **1965**, 2926. [b] Harned, H. S.; Embree, N. D. *J. Am. Chem. Soc.* **1934**, *56*, 1042. [c] Feldman, I.; Kovel, L. *Inorg. Chem.* **1963**, *2*, 145. [d] Lumme, P.; Laherno, P.; Tummavuori, J. *Acta Chem. Scand.* **1965**, *19*, 2175. [e] Jonassen, H. B.; LeBanc, R. B.; Meigohm, A. W.; Rogan, R. M. *J. Am. Chem. Soc.* **1950**, *72*, 2430. [f] Same value obtained for H_2(trien)$^{2+}$ (k_{2T} in Figure 2). [g] Units in s^{-1}.

Table VIII. General-Acid Rate Constants (k_{HB}, M^{-1} s^{-1}) for $Ni(H_{-2}GGHis)^-$ and $Ni(H_{-2}G_3)^-$

HB	$Ni(H_{-2}GGHis)^-$ [a]	$Ni(H_{-2}G_3)^-$ [b]
H_3O^+	*c*	9.5×10^4
H_2(glycinate)$^+$	$<5 \times 10^1$	1.1×10^4
HCOOH	4.7	5.8×10^2
HOAc	1.95	7.7×10^2
H_2O[d]	8×10^{-5}	8.6×10^{-2}

[a] 1.0 M $NaClO_4$. [b] See ref 3; 0.30 M $NaClO_4$. [c] Not detected. $k_{1H} << K_{1H}k_{1d}$ (=3×10^4 M^{-1} s^{-1}); see text. [d] Units in s^{-1}.

Two kinetic pathways (Figure 2) have been proposed for the acid dissociation reactions of metal-deprotonated peptide complexes.[1-4] (1) In the outside-protonation pathway (Scheme II), rapid protonation of the more basic peptide oxygen occurs prior to the rate-limiting breaking of the metal-peptide nitrogen bond. This pathway is specific acid catalyzed. (2) The inside-protonation pathway (Scheme I) occurs by direct proton transfer to the deprotonated peptide nitrogen. This pathway is subject to general-acid catalysis. The dissociation of $Ni(H_{-2}GGHis)^-$ complex is catalyzed by H_3O^+ as well as by general acids (HB). For the sake of simplicity in the preceding discussion, it was assumed that the H_3O^+-catalyzed reaction with $Ni(H_{-2}GGHis)^-$ proceeded solely by the outside-protonation pathway (eq 9, 10; Figure 2), although H_3O^+ could also be reacting by the inside-protonation pathway (eq 20). Previous investigations of the acid dissociation reactions of the deprotonated-peptide complexes of nickel(II) and copper(II) have been characterized by reaction mechanisms that involved only the specific-acid catalyzed outside-protonation pathway[2,5] or only the general-acid catalyzed inside-protonation (eq 20) pathway.[1,3,4,15,16] In all of the latter cases, the ratio of the rate constants (k_{1H}/k_{1HB}) for H_3O^+ and acetic acid is less than 500. However, for $Ni(H_{-2}GGHis)^-$ the ratio of k_{1H}/k_{1HB}, where k_{1H} is equal to $K_{1H}k_{1d}$, for acetic acid is greater than 10^4. The unusually high reactivity of H_3O^+ with $Ni(H_{-2}GGHis)^-$ as compared with that of acetic acid is attributed to the fact that the H_3O^+ reaction proceeds via the outside-protonation pathway (eq 9, 10; Figure 2), while acetic acid and other general acids react via the inside-protonation pathway (eq 20).

Summary

One or more of the nucleophilic outside-protonation, proton-assisted nucleophilic, proton-assisted general-acid, and inside-protonated pathways (Figure 2) have been shown to occur for other nickel(II)- and copper(II)-deprotonated peptide complexes;[1-9,15-17] however, $Ni(H_{-2}GGHis)^-$ is the first example of a deprotonated-peptide complex that can react by

---

(15) Pagenkopf, G. K.; Margerum, D. W. *J. Am. Chem. Soc.* **1968**, *90*, 501.
(16) Youngblood, M. P.; Chellappa, K. L.; Bannister, C. E.; Margerum, D. W. *Inorg. Chem.* **1981**, *20*, 1742.
(17) Wang, Y. H. C.; Margerum, D. W., to be submitted for publication.
(18) MES: 2-(*N*-morpholino)ethanesulfonic acid; PIPES, piperazine-*N*,*N'*-bis(2-ethanesulfonic acid). Good, N. E.; Winget, G. D.; Winter, W.; Connolly, T. N.; Izawa, S.; Singh, M. M. *Biochemistry* **1966**, *5*, 467.

all of the above mentioned pathways. The complexity of the $\mathrm{Ni(H_{-2}GGHis)^-}$ reactions arises because several of the pathways can simultaneously contribute to the rate of the observed dissociation reaction. Also, within each pathway, the location of the rate-determining step is very dependent on the reaction conditions.

At pH 5–7 the $\mathrm{Ni(H_{-2}GGHis)^-}$ complex reacts with acid and the rate expression contains both $[\mathrm{H^+}]^2$ and $[\mathrm{H^+}][\mathrm{HB}]$ terms. This is illustrated by the slope of -2 in Figure 1 and the complex acetic acid dependence in Figure 5. This kinetic behavior is accounted for by the proton-assisted general-acid reaction pathway in which the protonation of the $\mathrm{Ni(H_{-1}GGHis)}$ is rate limiting (D → E in Figure 2). When either or both of the general-acid and $\mathrm{H^+}$ concentrations is increased, the rate-limiting step is shifted to an earlier point in the reaction sequence. Under such circumstances the dissociation rate is carried by a combination of the inside-protonation and outside-protonation pathways. At higher $[\mathrm{H^+}]$ there is kinetic evidence for the formation of two outside-protonated species (D and C in Figure 2) with protonation constants of $10^{4.3}$ and $10^{1.3}$ $\mathrm{M^{-1}}$. Below pH 5 the dissociation reaction proceeds exclusively by the specific-acid catalyzed outside-protonation pathway (Figure 2). Even in the pH 5–7 region, $\mathrm{H_3O^+}$ preferentially reacts via the outside-protonation pathway, although general acids, HB, such as acetic acid react via the inside-protonation pathway (A → D in Figure 2). This conclusion is based on the observation that the ratio of the $\mathrm{H_3O^+}$ rate constant ($K_{1\mathrm{H}}k_{1\mathrm{d}}$) to the general-acid rate constants ($k_{1\mathrm{HB}}$) for the $\mathrm{Ni(H_{-2}GGHis)^-}$ reactions are more than 1 order of magnitude greater than has been observed for the reactions of $\mathrm{Ni(H_{-2}G_3)^-}$[1,4] and other metal–peptide complexes.[16,17]

The nucleophilic reaction of trien with $\mathrm{Ni(H_{-2}GGHis)^-}$ is more than 5 orders of magnitude slower than the analogous reaction with $\mathrm{Ni(H_{-2}G_3)^-}$. Furthermore, between pH 6 and pH 8 a proton-assisted nucleophilic pathway with $\mathrm{H_2(trien)^{2+}}$ is evident (Figure 2). In both of these respects the trien reactions with $\mathrm{Ni(H_{-2}GGHis)^-}$ are very similar to the analogous $\mathrm{Cu(H_{-2}GGHis)^-}$ reactions.[8,9]

Acknowledgment. This investigation was supported by National Science Foundation Grant CHE74-00043 and National Institutes of Health Grant GM19775.

Registry No. $\mathrm{Ni(H_{-2}GGHis)^-}$, 62006-82-0; trien, 112-24-3; glycine, 56-40-6; HCOOH, 64-18-6; HOAc, 64-19-7; $\mathrm{NH_2OH}$, 7803-49-8.

Contribution from the Department of Chemistry,
University of Houston, Houston, Texas 77004

Investigation of the Axial Ligand Binding Reactions of (*meso*-Tetraphenylporphinato)magnesium(II) with Nitrogenous Bases

K. M. KADISH* and L. R. SHIUE

Received June 15, 1981

The stability constants of the complexation reactions of (*meso*-tetraphenylporphinato)magnesium(II) ((TPP)Mg) with nitrogenous bases were calculated by the computer program SQUAD. This program processed the spectral data without any assumption; it provided more accurate results than those obtained from a Benesi–Hildebrand plot. The calculations yielded values for the stepwise stability constants of ML and $\mathrm{ML_2}$. The stability constants are linear functions of the ligand $\mathrm{p}K_\mathrm{a}$, which were similar to (TPP)Zn results. The different trends of log K_1 and log K_2 with the ligand $\mathrm{p}K_\mathrm{a}$ were explained.

Almost 30 years ago Miller and Dorough[1] measured the stability constants for addition of pyridine to (*meso*-tetraphenylporphinato)magnesium(II) ((TPP)Mg) in benzene. Fourteen years later a similar study was performed by Storm et. al.[2] using 2,6-lutidine as solvent. Two steps of axial ligand (L) addition to (TPP)Mg(M) are possible. The first step is the formation of the 1:1 complex (eq 1) and the second is the

$$\mathrm{M + L} \overset{K_1}{\rightleftharpoons} \mathrm{ML} \qquad \beta_1 = K_1 \tag{1}$$

1:2 complex (eq 2). Both studies found a close resemblance

$$\mathrm{ML + L} \overset{K_2}{\rightleftharpoons} \mathrm{ML_2} \qquad \beta_2 = K_1K_2 \tag{2}$$

of the optical absorption spectra between uncomplexed (TPP)Mg and the monopyridinate complex and observed that (TPP)Mg(py) was never completely converted to the dipyridinated complex $\mathrm{(TPP)Mg(py)_2}$. The facts that both the uncomplexed species and the monoadduct have almost identical spectra and that a very stable monopyridinate complex is followed by a very weak dipyridinate complex make calculations of stability constants from spectral curves difficult. Because of this difficulty, only a single value of ligand addition has ever been published for reaction 1 and reaction 2.

In our laboratory we have found a way to determine these stability constants by using a computer program, SQUAD (stability quotients from absorbance data).[3] This program has been set up to search for the best combination of stability constants that will describe the supplied data. A maximum of two metals, of two ligands, and of six unknown stability constants can be handled simultaneously by SQUAD and stability constants determined from small spectral differences between the complexed and uncomplexed species.

In this paper, we wish to present measured stability constants of (TPP)Mg complexed with 18 different nitrogenous bases under 0.1 M tetrabutylammonium perchlorate (TBAP) in methylene chloride ($\mathrm{CH_2Cl_2}$).

Experimental Section

Materials. Free base 5,10,15,20-tetraphenylporphyrin ($\mathrm{(TPP)H_2}$) was prepared by the method of Adler[4] and purified by the method of Barnett et al.[5] Mg(II) was inserted into $\mathrm{(TPP)H_2}$ by essentially the method of Adler et al.,[6] with $\mathrm{Mg(C_2H_3O_2)_2}$ in place of $\mathrm{MgCl_2}$

---

(1) Miller, J. R.; Dorough, G. D. *J. Am. Chem. Soc.* **1952**, *74*, 3977.
(2) Storm, C. B.; Corwin, A. H.; Arellano, R. R.; Martz, M.; Weintraub, R. *J. Am. Chem. Soc.* **1966**, *88*, 2525.
(3) Leggett, D. J.; McBryde, W. A. E. *Anal. Chem.* **1975**, *47*, 1065.
(4) Adler, A. D. *J. Org. Chem.* **1967**, *32*, 476.
(5) Barnett, G. H.; Hudson, M. F.; Smith, K. M. *J. Chem. Soc., Perkin Trans. 1* **1975**, *9*, 1401.